Triaxial deformation in ^{10}Be

N. Itagaki,[1,*] S. Hirose,[1] T. Otsuka,[1,2] S. Okabe,[3] and K. Ikeda[2]
[1]*Department of Physics, University of Tokyo, Hongo, Tokyo 113-0033, Japan*
[2]*The Institute of Physical and Chemical Research (RIKEN), Wako, Saitama 351-0198, Japan*
[3]*Center for Information and Multimedia Studies, Hokkaido University, Sapporo 060-0810, Japan*
(Received 15 September 2001; published 11 March 2002)

The triaxial deformation in ^{10}Be is investigated using a microscopic $\alpha+\alpha+n+n$ model. The states of two valence neutrons are classified based on the molecular-orbit (MO) model, and the π orbit is introduced about the axis connecting the two α clusters for the description of the rotational bands. There appear two rotational bands comprised mainly of $K^\pi=0^+$ and $K^\pi=2^+$, respectively, at low excitation energy, where the two valence neutrons occupy $K^\pi=3/2^-$ or $K^\pi=1/2^-$ orbits. The triaxiality and the K mixing are discussed in connection to the molecular structure, particularly to the spin-orbit splitting. The extent of the triaxial deformation is evaluated in terms of the electromagnetic transition matrix elements (Davydov-Filippov model, Q-invariant model) and density distribution in the intrinsic frame. The obtained values turned out to be $\gamma=15°-20°$.

DOI: 10.1103/PhysRevC.65.044302 PACS number(s): 21.10.−k, 21.60.Gx

I. INTRODUCTION

Recently, exotic structures of the Be isotopes have been theoretically and experimentally studied, and many new phenomena have been discussed [1–7]. One of them is the appearance of the cluster rotational band structure in the excited states of ^{10}Be ($\alpha+^6$He) [5,7] and ^{12}Be ($\alpha+^8$He, ^{6}He$+^6$He) [4,6]. We have suggested [8–10], based on the molecular-orbit (MO) model, that the development of α-α cluster structure depends on the neutron orbits located around the core comprised of α clusters. In the second 0^+ state of ^{10}Be, an anomalously prolonged α-α clustering structure emerges due to the valence neutrons located along the α-α axis [8,9].

The nucleus ^{10}Be has been known to have a strong β deformation due to the α-α core. In this paper, we discuss another aspect, a triaxial deformation. The triaxial deformation is possible as a result of the dynamics of the two valence neutrons. The triaxiality of ^{10}Be has been theoretically discussed based on the deformed oscillator model [11], in which a γ distortion of 34.8° has been predicted. According to the Davydov-Filippov model [12], this γ value suggests that the excitation energy of the second 2^+ state is 2.3 times higher than that of the first 2^+ state. In ^{10}Be, the first 2^+ state is observed at 3.358 MeV, and several 2^+ states have been observed around the 8 MeV region. Because of the presence of the 2^+ states in this energy region, recently, an experimental study has been performed in order to identify a triaxial structure of ^{10}Be [13].

In this paper, we discuss the triaxiality of ^{10}Be as a composite system of the α-α core and two valence neutrons, comparing it with other theoretical models. In our previous study on ^{10}Be [8], all of the observed low-lying positive- and negative-parity states are explained as combinations of three basic orbits ($K^\pi=3/2^-$, $1/2^+$, and $1/2^-$) of two valence neutrons around the two α clusters. Here, the z axis is taken to be the axis connecting two α clusters. If we adopt $K^\pi=3/2^-$ or $1/2^-$ orbits for the two valence neutrons, there appear two rotational bands in low energy; one is dominated by the $K=0$ intrinsic structure and the other by $K=2$. The calculated two 2^+ states of these bands can be related to the observed first 2^+ state at 3.358 MeV and the second 2^+ state at 5.958 MeV. It is therefore important to show how the triaxial intrinsic configuration emerges in these states, and how the orbits of the valence neutrons deviate from the axial symmetry. Here, we calculate the electro-magnetic transition between these $K=0$ and $K=2$ bands [$B(E2; K=2\rightarrow K=0)$] as a signal of a triaxial deformation. This transition is suppressed when the orbitals are of pure axial symmetry. However, the orbitals may deviate from the axial symmetry, when the valence neutrons are mutually more correlated and form a localized dineutron pair due to the neutron-neutron interaction. The recoil effect of the valence neutrons with respect to the α-α core then plays a role to break the axial symmetry of the charge distribution.

This paper is organized as follows. In Sec. II, we give a description of the single-particle orbits around the two α clusters based on MO. In Sec. III, we show our results on ^{10}Be, and a conclusion is given in Sec. IV.

II. EXTENDED MOLECULAR-ORBIT MODEL

The framework is the same as in Ref. [8], and only important points are recaptured here. We introduce a microscopic $\alpha+\alpha+2n$ model for ^{10}Be. The neutron configurations are introduced based on the molecular orbit (MO) picture [14–16]. The total wave function is fully antisymmetrized and expressed as a superposition of Slater determinants with various configurations of the valence neutrons. The Slater determinants are also superposed with respect to different relative distances between the two α clusters. The projection to the eigenstates of angular momentum J is numerically performed. All nucleons are described by Gaussians with a common oscillator parameter. Two α clusters are introduced on the z axis, and the wave function of the ith

*Electronic address: itagaki@phys.s.u-tokyo.ac.jp

valence neutron ($\phi_i\chi_i$) is expressed by a linear combination of local Gaussians:

$$\phi_i\chi_i=\sum_j g_j G_{R_j}\chi_i, \tag{1}$$

where $\vec{R}_j$ is a parameter corresponding to the Gaussian center.

In the MO model, the states of the valence neutrons are expressed by a linear combination of orbits around two α clusters. The lowest orbit has one node and negative parity, that is the p orbit. We take the harmonic-oscillator-type wave function for the p orbit. Such p orbits in the x, y, and z direction are denoted as ψ_x, ψ_y, and ψ_z, respectively. We now classify single-particle orbits for the valence neutrons in terms of K quantum numbers:

$$\psi_x+i\psi_y=(x+iy)\exp[-\nu r^2]\propto rY_{11}\exp[-\nu r^2], \tag{2}$$

$$\psi_z=z\exp[-\nu r^2]\propto rY_{10}\exp[-\nu r^2], \tag{3}$$

$$\psi_x-i\psi_y=(x-iy)\exp[-\nu r^2]\propto rY_{1-1}\exp[-\nu r^2]. \tag{4}$$

These p orbits have $K=1$, 0, and -1, respectively.

Now we construct MO from these p orbits. Since each valence neutron can move around one of the two α clusters, there should be two sets of the p orbits defined with respect to those two α clusters. Thus, the $(\psi_x\pm i\psi_y)$ orbit whose center is shifted at $+a[-a]$ on the z axis is denoted as $(\psi_x\pm i\psi_y)_{+a}$ $[(\psi_x\pm i\psi_y)_{-a}]$. As linear combinations of these orbits, the lowest MOs are expressed as

$$\psi_1^{\mathrm{MO}}=(\psi_x+i\psi_y)_{+a}+(\psi_x+i\psi_y)_{-a}, \tag{5}$$

$$\psi_{-1}^{\mathrm{MO}}=(\psi_x-i\psi_y)_{+a}+(\psi_x-i\psi_y)_{-a}. \tag{6}$$

These orbits clearly have $K=1$ and $K=-1$, respectively. In these cases, the classical picture of p orbit is a circular motion about the α-α (z) axis. This is the so-called π orbit.

If we take a linear combination of $(\psi_z)_{+a}$ and $(\psi_z)_{-a}$, the orbit becomes the so-called σ orbit, just along the α-α (z) axis. This orbit is a higher-nordal orbit and only relevant to the second 0^+ state, discussed also in antisymmetrized molecular dynamics (AMD) calculations [17] and in stochastic variational method (SVM) calculations [18]. We now disregard this orbit.

These $(\psi_x)_{+a}$, $(\psi_x)_{-a}$, $(\psi_y)_{+a}$, and $(\psi_y)_{-a}$ orbits can be approximated by a combination of two local Gaussians, whose centers are shifted by a variational parameter b perpendicular to the z axis. We thus use the following wave functions:

$$(\psi_x)_{+a}\propto G_{a\vec{e}_z+b\vec{e}_x}-G_{a\vec{e}_z-b\vec{e}_x},$$

$$(\psi_y)_{+a}\propto G_{a\vec{e}_z+b\vec{e}_y}-G_{a\vec{e}_z-b\vec{e}_y},\ \ldots\ . \tag{7}$$

The values of these parameters a and b are variationally determined by using the cooling method in AMD [19–24] independently for each α-α distance. Since the rotational symmetry about the z axis is broken with Eq. (10), the wave functions do not have exactly conserved quantum number K. On the other hand, the parameter b is small enough usually, and the K^π number is preserved to a good extent, and is expressed hereafter as $\overline{K^\pi}$.

When these orbital parts of the wave functions are coupled with the spin part, the orbits with $\overline{K^\pi}=3/2,\ 1/2,\ -1/2$, and $-3/2$ are introduced as follows:

$$|3/2^-\rangle=\psi_1^{\mathrm{MO}}|n\uparrow\rangle,\quad |1/2^-\rangle=\psi_1^{\mathrm{MO}}|n\downarrow\rangle, \tag{8}$$

and their time reversal,

$$|-3/2^-\rangle=\psi_{-1}^{\mathrm{MO}}|n\downarrow\rangle,\quad |-1/2^-\rangle=\psi_{-1}^{\mathrm{MO}}|n\uparrow\rangle. \tag{9}$$

Using these orbits, we introduce three configurations of $\Phi((3/2^-)^2)$ with $\overline{K}=0$, $\Phi((1/2^-)^2)$ with $\overline{K}=0$, and $\Phi(3/2^-\ 1/2^-)$ with $\overline{K}=2$ for the two valence neutrons, and mixing amplitude of these configurations are variationally determined after the angular momentum projection.

The Hamiltonian and the effective nucleon-nucleon interaction used are the same as in Ref. [8].

III. TRIAXIAL STRUCTURE IN ^{10}Be

In ^{10}Be, we adopt three configurations $\Phi((3/2^-)^2)$, $\Phi((1/2^-)^2)$, and $\Phi(3/2^-\ 1/2^-)$. The values of the parameters for the valence neutrons are obtained variationally. The parameter a describes the positions of the Gaussian centers on the α-α (z) axis, and parameter b corresponds to the rotation radius of the π orbit about the α-α axis. The optimized values are listed in Ref. [8].

Before performing the angular momentum projection, we discuss the triaxial deformation of the intrinsic wave function. The intrinsic density of $\Phi((3/2^-)^2)$ is shown in Fig. 1 [(a), xz plane; (b), xy plane], where the α-α distance is chosen to be optimal, as it turns out to be 3 fm.

The intrinsic density is defined as a snapshot of a rotating system. The plane in which the spin-up valence neutrons stays at a given moment is defined as the xz plane, with the z axis being the α-α axis. Therefore, the spin-up valence neutron is fixed on the xz plane, and the spin-down valence neutron occupy the normal $\overline{K}=-3/2^-$ orbit. The intrinsic density on the xz plane [Fig. 1(a)] shows a large β deformation along the z axis due to the presence of two α clusters. As for the xy plane [Fig. 1(b)], as you can naively expect, the density shows deviation from circular distribution and mixture of a triaxial component is evident. The contour line of 0.01 in Figs. 1(a) and 1(b) suggests the deformation of this nucleus is $\beta\sim0.5$ and $\gamma=11°$.

We then perform the angular momentum projection, where the wave function is rotated and integrated over the Euler angle, and the rotational symmetry is restored. Here, the K mixing between $K=0$ and $K=2$ finally determines the degree of the triaxiality of the system.

This intrinsic wave function is numerically projected to the eigenstates of angular momentum, and the basis states are superposed by generator coordinate method (GCM). Here, the coefficients representing linear combinations of Gaussians for each single particle orbit are treated as varia-

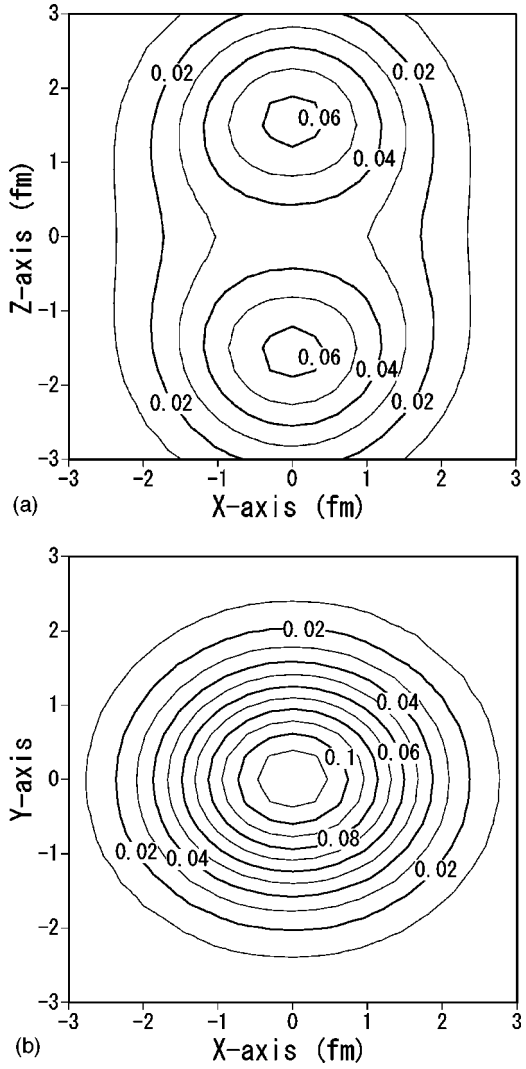

FIG. 1. The intrinsic density of $\Phi((3/2^-)^2)$ [(a) xz plane; (b) xy plane], where the α-α distance is chosen to be optimal 3 fm.

tional parameters to take into account deviations from the original orbits. Because of this, not only the ''single-particle'' MO state where the valence neutrons independently rotate around the α-α core, but also more complex states where the valence neutrons are mutually more correlated as a dineutron cluster can be included.

Using our framework, the binding energy of one α cluster is calculated to be 27.5 MeV, and the threshold energy of free $\alpha+\alpha+n+n$ system is $2\times(-27.5)=-55.0$ MeV. Experimentally, the ground state is lower than this energy by 8.4 MeV.

As $K=0$ levels, the ground 0^+ state is calculated at -60.5 MeV, the 2^+ state appears at $E_x=3.6$ MeV, and the 4^+ state appears at $E_x=12.9$ MeV. They fit quite well into the $J(J+1)$ rule, and the dominant component is $(3/2^-)^2$ for the two valence neutrons. As $K=2$ states, the 2^+ state at $E_x=5.6$ MeV, the 3^+ state at $E_x=9.4$ MeV, and the 4^+ state at $E_x=14.4$ MeV form a rotational band structure. They also fit quite well into the $J(J+1)$ rule. The $K=2$ band dominantly has a component of $(3/2^-)(1/2^-)$ for the two valence neutrons, where one of them feels the spin-orbit interaction attractively and the other feels it repulsively. After the mixing of these two bands, the first 2^+ state becomes $E_x=3.1$ MeV (experimentally 3.358 MeV), and the second one is slightly pushed up ($E_x=5.6$ MeV, experimentally 5.958 MeV). The first 2^+ state has the squared overlap with the $K=0$ state by 0.96, and the second 2^+ state has the squared overlap with the $K=2$ state by 0.92. Therefore, the second 2^+ state has the component of $K=0$ by 8%, and it can be considered as an indication of a triaxial deformation.

TABLE I. The electromagnetic transition probability $[B(E2)]$ in ^{10}Be after K mixing. All units are in e^2 fm^4.

$B(E2;\ 2_1^+\rightarrow 0_1^+)$	11.8 (expt. 10.04 ± 1.2)
$B(E2;\ 2_2^+\rightarrow 0_1^+)$	0.70
$B(E2;\ 2_1^+\rightarrow 2_2^+)$	3.99
$B(E2;\ 4_2^+\rightarrow 2_1^+)$	11.1

This triaxiality of the 2^+ states is reflected in the electromagnetic transition rate, and $B(E2)$ values are summarized in Table I.

The $E2$ transition between the first 2^+ state and the ground state is calculated as $B(E2;\ 2_1^+\rightarrow 0_1^+)=11.8\ e^2$ fm^4, which agrees with the experimental value of $10.04\pm 1.2\ e^2$ fm^4. Furthermore, the inter-band transition is calculated: $B(E2;\ 2_1^+\rightarrow 2_2^+)=3.99\ e^2$ fm^4. If the system is axially symmetric, this transition between different K values is more suppressed. Therefore, the value indicates that the 2^+ states have a component of a triaxial deformation.

Using the Davydov-Filippov model [12], we can estimate the degree of the triaxiality as a function of the γ angle. The ratios $B(E2;\ 2_2^+\rightarrow 0_1^+)/B(E2;\ 2_1^+\rightarrow 0_1^+)$ and $B(E2;\ 2_2^+\rightarrow 2_1^+)/B(E2;\ 2_1^+\rightarrow 0_1^+)$ are given in the Davydov-Filippov model as follows:

$$\frac{B(E2;\ 2_2^+\rightarrow 0_1^+)}{B(E2;\ 2_1^+\rightarrow 0_1^+)}=\frac{1-\dfrac{3-2\sin^2(3\gamma)}{\sqrt{9-8\sin^2(3\gamma)}}}{1+\dfrac{3-2\sin^2(3\gamma)}{\sqrt{9-8\sin^2(3\gamma)}}}, \tag{10}$$

$$\frac{B(E2;\ 2_2^+\rightarrow 2_1^+)}{B(E2;\ 2_1^+\rightarrow 0_1^+)}=\frac{\dfrac{20}{7}\dfrac{\sin^2(3\gamma)}{9-8\sin^2(3\gamma)}}{1+\dfrac{3-2\sin^2(3\gamma)}{\sqrt{9-8\sin^2(3\gamma)}}}. \tag{11}$$

These values are compared with our calculation in Fig. 2. The solid line in Fig. 2 shows the ratio $B(E2;\ 2_2^+\rightarrow 2_1^+)/B(E2;\ 2_1^+\rightarrow 0_1^+)$ calculated with the Davydov-Filippov model. The ratio becomes 0.34 in our calculation, and it has a crossing point with the Davydov-Filippov model around $\gamma=19°$. The dotted line in Fig. 2 shows the ratio $B(E2;\ 2_2^+\rightarrow 0^+)/B(E2;\ 2_1^+\rightarrow 0_1^+)$ calculated with the Davydov-Filippov model, and it crosses with our result of 0.059 around $\gamma=17°$ and 22°. These results strongly suggest that ^{10}Be has a triaxial deformation of $\gamma=15°$–$20°$. Although the α-α core is of axial symmetry and electric charge

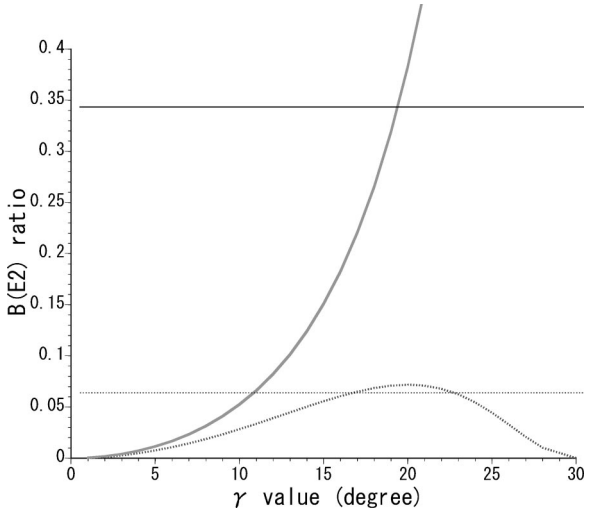

FIG. 2. $B(E2)$ ratios $B(E2;\ 2_2^+ \rightarrow 2_1^+)/B(E2;\ 2_1^+ \rightarrow 0_1^+)$ (solid line) and $B(E2;\ 2_2^+ \rightarrow 0_1^+)/B(E2;\ 2_1^+ \rightarrow 0_1^+)$ (dotted line), as a function of γ (degree). Our results of 0.34 and 0.059 cross with the Davydov-Filippov model around 15°~20°.

are only in the α's, the recoil effect gives rise to a change from the axial symmetry to the triaxial shape.

The γ value can be deduced also in terms of Q-invariant model. In Ref. [25], the γ value is related to the reduced matrix elements of Q operator:

$$q_2 = \sum_i \langle 0_1^+ || Q || 2_i^+ \rangle \langle 2_i^+ || Q || 0_1^+ \rangle, \tag{12}$$

$$q_3 = \sqrt{\frac{7}{10}} \sum_{i,j} \langle 0_1^+ || Q || 2_i^+ \rangle \langle 2_i^+ || Q || 2_j^+ \rangle \langle 2_j^+ || Q || 0_1^+ \rangle, \tag{13}$$

$$\frac{q_3}{{q_2}^{3/2}} = \cos 3\gamma. \tag{14}$$

Using these relations and taking the sum over indices i and j up to 2, our calculated results correspond to $\gamma = 20.1°$.

We discuss the electromagnetic transition between the two 2^+ states (K-mixing effect between the two 2^+ states) by artificially changing the strength parameter V_0^{ls} in Ref. [8] for the spin-orbit term. The Majorana parameter M for the central term is simultaneously changed to keep the calculated ground 0^+ state energy constant. In Table II, the $B(E2;\ 2_1^+ \rightarrow 2_2^+)$ values are listed together with the calculated energies and magnetic dipole moments. Using the original interaction, the $B(E2;\ 2_1^+ \rightarrow 2_2^+)$ value is predicted as 3.99 e^2 fm^4.

When we increase the V_0^{ls} value, the excitation energy of the second 2^+ state becomes higher, since one of the valence neutrons repulsively feels the spin-orbit interaction. The original interaction ($V_0^{ls} = 2000$ MeV and $M = 0.6$) gives $E_x = 5.70$ MeV for the 2_2^+ state, but the interaction with $V_0^{ls} = 2500$ MeV and $M = 0.61$ gives $E_x = 6.82$ MeV. The $B(E2;\ 2_1^+ \rightarrow 2_2^+)$ value then decreases from 3.99 e^2 fm^4 to 2.20 e^2 fm^4. Therefore, it is considered that with increasing LS strength, the K quantum number of each 2^+ state approaches a good number, where the $E2$ transition between the two 2^+ states is suppressed. On the other hand, when the spin-orbit interaction becomes weaker, the transition rapidly increases. The V_0^{ls} value of 1500 MeV gives the $B(E2;\ 2_1^+ \rightarrow 2_2^+)$ values of 9.53 e^2 fm^4, and when we adopt $V_0^{ls} = 1000$ MeV, the value becomes 17.53 e^2 fm^4. Here, the orbits of the valence neutrons deviate from ones with good K quantum numbers, and a triaxial $\alpha + \alpha +$dineutron clustering configuration where the two valence neutrons are strongly correlated becomes important.

We can intuitively interpret this behavior as follows: when the spin-orbit interaction is weak enough, the two valence neutrons form a dineutron, in which the attractive interaction between them strongly contributes. However, when the spin-orbit interaction acts significantly and becomes more important, the dineutron pair is broken and each va-

TABLE II. The electromagnetic transition probability $[B(E2)]$ from the first 2^+ state to second 2^+ state calculated by changing the strength of the spin-orbit interaction (V_0^{ls}). The Majorana parameter (M) for the central interaction is also changed to keep the calculated ground 0^+ state energy constant. The original interaction is $V_0^{ls} = 2000$ MeV and $M = 0.6$. The magnetic dipole moment is also predicted. $\mu(pl)$ and $\mu(ns)$ represent proton-orbital part and neutron-spin part, respectively.

V_0^{ls} (MeV)	1000	1500	2000	2500
M	0.58	0.59	0.60	0.61
0_1^+ (MeV)	−60.48	−60.38	−60.51	−60.75
2_1^+ (MeV)	−57.69	−57.30	−57.26	−57.33
2_2^+ (MeV)	−56.71	−55.78	−54.88	−53.93
$B(E2;\ 2_1^+ \rightarrow 2_2^+)(e^2\ \mathrm{fm}^4)$	17.53	9.53	3.99	2.20
$\mu(2_1^+)$ (μ_N)	0.57	0.73	0.72	0.69
$(\mu(pl),\ \mu(ns))$	(0.70, −0.13)	(1.04, −0.30)	(1.13, −0.41)	(1.16, −0.48)
$\mu(2_2^+)$ (μ_N)	0.91	0.59	0.48	0.43
$(\mu(pl),\ \mu(ns))$	(1.03, −0.12)	(0.65, −0.06)	(0.51, −0.04)	(0.46, −0.03)

lence neutron rotates around the core in opposite direction with definite K values. Note that the spin-orbit interaction does not act to form a dineutron pair with $S=0$. This is close to the jj-coupling picture and axial symmetry of the system is restored.

This situation can be interpreted also from the nuclear SU_3 model. At the SU_3 limit (parameters a, b, and $d\rightarrow 0$), $\Phi((3/2^-)^2)$ (dominant configuration of 2_1^+) and $\Phi(3/2^-\ 1/2^-)$ (dominant configuration of 2_2^+) correspond to linear combinations of two SU_3 configurations: $(n_x,n_y,n_z)=(2,0,4)$, $(\lambda,\mu)=(2,2)$ and $(n_x,n_y,n_z)=(1,1,4)$, $(\lambda,\mu)=(3,0)$ ($n_z=4$ is due to the α clusters along the z axis). This is because the valence neutrons in $3/2^-$ and $1/2^-$ are expressed as linear combinations of p orbitals along the x and y direction. Here, the spin-orbit interaction determines the mixing ratio of the two SU_3 representations. When it is strong enough, since the jj-coupling picture works well, these two configurations are mixed to the almost same amount. However, when the spin-orbit interaction is weakened, the binding-energy gain due to the mixing amplitudes changes. Here, the $(\lambda,\mu)=(2,2)$ configuration, which is a dineutron configuration, becomes much more important than the $(\lambda,\mu)=(3,1)$ configuration. This means that a triaxial deformation is induced when the spin-orbit interaction becomes weaker.

Next, we examine the magnetic dipole moment as a probe to determine the strength of the spin-orbit interaction. In Table II, the magnetic dipole moments of these two 2^+ states are listed, and we predict $\mu=0.72\mu_N$ and $0.48\mu_N$ for the first and the second 2^+ states, respectively. Unfortunately, the dependence of the total magnetic moment of these states with respect to the spin-orbit strength is rather monotonic. However, each component has a significant dependence. In Table II, the proton-orbital part and the neutron-spin part are also listed (the neutron-orbital part is, of course, zero, and the proton-spin part also becomes zero due to the assumption of the α clusters).

As for the proton-orbital part, using the original interaction ($V_0^{ls}=2000$ MeV,$M=0.6$), 2_1^+ is calculated to have a larger value than 2_2^+: the 2_1^+ state has $1.13\mu_N$ and the 2_2^+ state has $0.46\mu_N$. The 2_1^+ state is mainly of $K=0$, and therefore the rotation of the α-α core is the main source of the angular momentum ($J=2$). However, in the case of 2_2^+, since the valence neutrons already have $K=2$, the rotation of α-α is not necessary to construct $J=2$, and hence the proton-orbital part is smaller than 2_1^+. These values depend on the strength of the spin-orbit interaction. With decreasing spin-orbit strength, the difference of proton-orbital part between these two states becomes smaller due to increase of the K-mixing effect between the two 2^+ configurations, which we discussed. When the strength of the spin-orbit interaction is $V_0^{ls}=1500$ MeV, 2_1^+ has $1.04\mu_N$ and 2_2^+ has $0.65\mu_N$. As for the neutron-spin part, in the $V_0^{ls}=2000$ MeV case (original interaction), 2_1^+ has $-0.41\mu_N$ and 2_2^+ has $-0.04\mu_N$. This result suggests that the 2_1^+ state has both spin-singlet and spin-triplet components of the valence neutrons. The 2_2^+ state is dominated by the spin-singlet component. In the 2_2^+ state, one of the valence neutrons repulsively feels the spin-orbit interaction, and when the two valence neutrons construct a spin singlet, it helps to reduce the contribution of the repulsive spin-orbit interaction. This is the main reason for the smaller neutron-spin part in 2_2^+. On the other hand, if we use weaker spin-orbit strength, the difference of the neutron-spin part between the two 2^+ states becomes much smaller. When the strength of the spin-orbit interaction is $V_0^{ls}=1000$ MeV, 2_1^+ has $-0.13\mu_N$ and 2_2^+ has $-0.12\mu_N$.

Finally, we comment that the K-mixing effect is also important for the 4^+ states. The 4^+ state with $K=0$ at $E_x=12.9$ MeV becomes $E_x=10.5$ MeV after the K mixing, and the 4^+ state with $K=2$ at $E_x=14.4$ MeV is pushed up to $E_x=17.0$ MeV. The first 4^+ state has the squared overlap of 0.78 with the $K=0$ state and 0.63 with the $K=2$ state (here, $K=0$ and $K=2$ are not orthogonal). Therefore, the first 4^+ state has almost an equal contribution of the $K=0$ and the $K=2$ basis states. This is because, in the case of 4^+, the angular momentum vector with $K=0$ and $K=2$ are not necessary to be spatially orthogonal, which is different from the case of 2^+. Therefore, the K mixing for the 4^+ state of ^{10}Be is very strong, and the electromagnetic transition probability for the yrast band deviates from a simple rigid-body picture. The $B(E2;\ 4_1^+\rightarrow 2_1^+)$ value is calculated to be 11.1 e^2 fm^4, even smaller than the $B(E2;\ 2_1^+\rightarrow 0_1^+)$ value of 11.8 e^2 fm^4, and the $B(E2;\ 4_1^+\rightarrow 2_1^+)/B(E2;\ 2_1^+\rightarrow 0_1^+)$ ratio of 0.94 much deviates from the rigid-body limit of 1.43. If we restrict the model space to $K=0$, then the $B(E2;\ 4_1^+\rightarrow 2_1^+)$ becomes 14.7 e^2 fm^4, and the ratio $B(E2;\ 4_1^+\rightarrow 2_1^+)/B(E2;\ 2_1^+\rightarrow 0_1^+)$ of 1.18 becomes closer to 1.43. In the nuclear SU_3 model, the 4^+ states with $K=0$ $[(\lambda,\mu)=(2,2)]$ and $K=2$ $[(\lambda,\mu)=(3,1)]$ become the same representation. This character partially remains as a strong K-mixing effect in the present MO model.

IV. SUMMARY AND CONCLUSION

We have applied the $\alpha+\alpha+n+n$ model to ^{10}Be and discussed the triaxial deformation of this nucleus. The orbits for the valence neutrons have been introduced based on the molecular orbit (MO) model. In the present model, the spatially extended motion of the valence neutrons around the α clusters are described by linear combinations of Gaussians, and the centers of the Gaussians are variationally determined.

The calculated energy levels show the appearance of two band structures, which have dominantly $K=0$ and $K=2$ components, when the two valence neutrons occupy $K^\pi=3/2^-$ or $K^\pi=1/2^-$ orbits. The first 2^+ state has the squared overlap with the $K=0$ state by 0.96, and the second 2^+ state has the squared overlap with the $K=2$ state by 0.92. Since the second 2^+ state has the component of $K=0$ by 8%, the electromagnetic transition from the 2_1^+ state (mainly $K=0$) to the 2_2^+ state (mainly $K=2$) is allowed (3.99 e^2 fm^4). Using the Davydov-Filippov model [12], we estimated the triaxiality for the 2^+ state. The ratio $B(E2;\ 2_2^+\rightarrow 2_1^+)/B(E2;\ 2_1^+\rightarrow 0_1^+)$ calculated with the Davydov-Filippov model and our model coincide around $\gamma=19°$, and the $B(E2)$ ratio $B(E2;\ 2_2^+\rightarrow 0^+)/B(E2;\ 2_1^+\rightarrow 0_1^+)$ indicates $\gamma=17°-22°$. Originally, the α-α core is introduced to be of

axial symmetry. However, because of the recoil effect of the valence neutrons, the charge distribution deviates from the axial symmetry, and the system becomes triaxial. We also discussed the triaxial deformation by artificially weakening the spin-orbit interaction. With decreasing spin-orbit interaction, the orbits of the valence neutrons deviate from the jj-coupling limit, and the dineutron configuration becomes important. Here, the system becomes three-body-like and the $B(E2;\ 2_2^+ \rightarrow 2_1^+)$ value drastically increases.

Similar dineutron components are discussed in weakly bound systems with the so-called halo structure. For example, in ^{6}He, in addition to the shell-model-like space, the model space of dineutron$+\,^4$He has been shown to be important [26]. This means that a locally correlated dineutron wave function is important for the description of the valence neutrons with small binding energy and spatially extended distribution. It is consistent with our discussion on the effect of varying the strength of the spin-orbit interaction. Namely, when the valence neutrons with low binding energies have a halo structure, the contribution of the spin-orbit interaction between the core and the valence neutrons becomes weak. Here, the valence neutrons form a dineutron pair with spin singlet, by which they can increase the spatial overlap between them and the contribution of the attractive interaction. Therefore, it is very challenging to explore the triaxial deformations in ^{12}Be and ^{14}Be, which have weakly bound neutrons and also deformed cores.

ACKNOWLEDGMENTS

The authors thank members of Nuclear Theory group in University of Tokyo and RI beam science laboratory in RIKEN for discussions and encouragements. They also thank Dr. I. Kumagai-Fuse for her help. One of the authors (N.I.) thanks Professor R. Lovas, Professor W. von Oertzen, Professor H. Horiuchi, Professor K. Katō, and Dr. Y. Kanada-En'yo for fruitful discussions. This work was supported in part by Grant-in-Aid for Scientific Research (13740145) from the Ministry of Education, Science and Culture.

[1] H. Iwasaki *et al.*, Phys. Lett. B **481**, 7 (2000).
[2] H. Iwasaki *et al.*, Phys. Lett. B **491**, 8 (2000).
[3] A. Navin *et al.*, Phys. Rev. Lett. **85**, 266 (2000).
[4] A. A. Korscheninnikov *et al.*, Phys. Lett. B **343**, 53 (1995).
[5] N. Soić *et al.*, Europhys. Lett. **34**, 7 (1996).
[6] M. Freer *et al.*, Phys. Rev. Lett. **82**, 1383 (1999).
[7] M. Freer *et al.*, Phys. Rev. C **63**, 034301 (2001).
[8] N. Itagaki and S. Okabe, Phys. Rev. C **61**, 044306 (2000).
[9] N. Itagaki, S. Okabe, and K. Ikeda, Phys. Rev. C **62**, 034301 (2000).
[10] N. Itagaki, S. Okabe, K. Ikeda, and I. Tanihata, Phys. Rev. C **64**, 014301 (2001).
[11] M. Harvey and F. C. Khanna, in *Nuclear Spectroscopy and Reactions*, Part D: *Models of Light Nuclei*, edited by J. Cerny (Academic Press, New York, 1975), p. 69.
[12] A.S. Davydov and G.F. Filippov, Nucl. Phys. **8**, 237 (1958).
[13] N. Curtis *et al.*, Phys. Rev. C **64**, 044604 (2001).
[14] Y. Abe, J. Hiura, and H. Tanaka, Prog. Theor. Phys. **49**, 800 (1973).
[15] H. Furutani, H. Kanada, T. Kaneko, S. Nagata, H. Nishioka, S. Okabe, S. Saito, T. Sakuda, and M. Seya, Suppl. Prog. Theor. Phys. **68**, 193 (1980).
[16] M. Seya, M. Kohno, and S. Nagata, Prog. Theor. Phys. **65**, 204 (1981).
[17] Y. Kanada-En'yo, H. Horiuchi, and A. Doté, Phys. Rev. C **60**, 064304 (1999).
[18] Y. Ogawa, K. Arai, Y. Suzuki, and K. Varga, Nucl. Phys. **A673**, 122 (2000).
[19] Y. Kanada-En'yo and H. Horiuchi, Prog. Theor. Phys. **93**, 115 (1995).
[20] Y. Kanada-En'yo, H. Horiuchi, and A. Ono, Phys. Rev. C **52**, 628 (1995).
[21] Y. Kanada-En'yo and H. Horiuchi, Phys. Rev. C **52**, 647 (1995).
[22] A. Doté, H. Horiuchi, and Y. Kanada-En'yo, Phys. Rev. C **56**, 1844 (1997).
[23] A. Ono, H. Horiuchi, T. Maruyama, and A. Ohnishi, Prog. Theor. Phys. **87**, 1185 (1992); Phys. Rev. Lett. **68**, 2898 (1992).
[24] S. Okabe and Y. Abe, Prog. Theor. Phys. **61**, 1049 (1979).
[25] V. Werner, N. Pietralla, P. von Brentano, R.F. Casten, and R.V. Jolos, Phys. Rev. C **61**, 021301(R) (2000).
[26] S. Aoyama, S. Mukai, K. Katō, and K. Ikeda, Prog. Theor. Phys. **93**, 99 (1995).